

Document downloaded from:

<http://hdl.handle.net/10251/84578>

This paper must be cited as:

Galindo, J.; Climent, H.; Tiseira Izaguirre, AO.; García-Cuevas González, LM. (2016). Effect of the numerical scheme resolution on quasi-2D simulation of an automotive radial turbine under highly pulsating flow. *Journal of Computational and Applied Mathematics*. 291:112-126. doi:10.1016/j.cam.2015.02.025.



The final publication is available at

<http://dx.doi.org/10.1016/j.cam.2015.02.025>

Copyright Elsevier

Additional Information

Effect of the numerical scheme resolution on quasi-2D simulation of an automotive radial turbine under highly pulsating flow

J. Galindo^a, A. Tiseira^a, H. Climent^a, L.M. García-Cuevas^{a,*}

^a*CMT-Motores Térmicos, Universitat Politècnica de València, Valencia 46022, Spain.*

Abstract

Automotive turbocharger turbines usually work under pulsating flow because of the sequential nature of engine breathing. However, existing turbine models are typically based on quasi-steady assumptions. In the paper a model where the volute is calculated in a quasi-2D scheme is presented. The objective of the work is to quantify and analyse the effect of the numerical resolution scheme used in the volute model. The conditions imposed upstream are isentropic pressure pulsations with different amplitude and frequency. The volute is computed using a finite volume approach considering the tangential and radial velocity components. The stator and rotor are assumed to be quasi-steady. In the paper, different integration and spatial reconstruction schemes are explored. The spatial reconstruction is based on the MUSCL method with different slope limiters fulfilling the TVD criterion. The model results are assessed against 3D U-RANS calculations. The results show that under low frequency pressure pulses all the schemes lead to similar solutions. But, for high frequency pulsation the results can be very different depending upon the selected scheme. This may have an impact in noise emission predictions.

1. Introduction

Nowadays internal combustion engines, ICE, are facing two main problems, the pollutants emission and the fuel consumption reduction, in order to fulfill new regional regulations such as the European norm Euro VI [1], [2] while maintaining the engine performance. The new engine design paradigm used to reach these objectives is based in a reduction of the engine size while incrementing the inlet pressure, an action known as downsizing. This is usually done using a turbocharger placed in the intake and in the exhaust line, and engine efficiency is highly affected by the turbocharger efficiency.

0-D models can be used to compute the turbine behaviour coupled with an engine. These models can predict the flow characteristics at low engine regimes and pulse frequencies, when wave effects are small and the main effects are due to mass and energy accumulation in the volute, as shown in [3] and [4]. At higher engine regimes and pulse frequencies, however, wave effects become important and 0-D models fall short in accuracy, so one-dimensional codes are used instead. Engine manufacturers are growing their usage of one-dimensional codes during engine development, as they provide accurate results while keeping their computational costs low enough to be used during intensive and broad simulation campaigns. As pulsating flow becomes more important with further engine downsizing and urban driving emission regulations become more stringent, the importance of one-dimensional accurate predictions of turbocharger performances under high amplitude and frequency

boundary conditions grow in importance. In one-dimensional codes, the main wave-action effects are supposed to happen in the volute, as it is the largest element of the turbine, just as is observed in CFD simulations [5]. The volute is solved as an equivalent one-dimensional duct of a given length and area distribution, what can be called a classical one-dimensional volute model. The main philosophy behind these models is shown in [6], where the volute is modelled using two tapered pipes. The first tapered pipe represents the turbine inlet duct, from the very beginning of the turbine to the volute tongue, with a length, inlet diameter and outlet diameter equal to the real ones. The second duct had a length equal to the length of the volute from the tongue to a point at 180°, passing through the central point of each section, setting the duct area to get the correct volute volume. This length selection was done supposing that half the mass flow enters the rotor at this point. This method is further refined and used in other works, such as in the work by Abidat et al. [7] and by Costall et al. [8]. The accuracy of this one-dimensional approach is limited for frequencies higher than 1000 Hz, and it is expected that a more realistic simulation of the volute, taking into account its lateral window flow, should provide better results. Chiong et al. [9] present a volute with some of its cells directly connected to the rotor inlet in a quasi-bidimensional approach, providing good results. Galindo Lucas et al. [10] present a quasi-bidimensional model where each volute cell is connected to the stator nozzles, showing promising results for high frequencies. Several numerical schemes for solving the last model can be used, and they are analysed in this work.

State of the art one-dimensional engine simulation codes are becoming fast enough to attain speeds between 1% and 5% of real-time for realistic engines and running in commod-

*Corresponding author. Tel: +34963877650; fax: +34963877659
Email address: luiga12@mot.upv.es (L.M. García-Cuevas)
URL: www.cmt.upv.es (L.M. García-Cuevas)

ity hardware, so they seem a viable alternative for HIL experiments in a not so distant future. Algorithm improvements should speed up current codes, and upgrades in SIMD operations as the rise from 4 double precision to 8 double precision floating point operations (FLOP) per cycle seen in the last generations of x86 processors, will provide means to reduce the time needed to achieve the goal of HIL simulation of a full engine with wave-action effects. The optimum selection of numerical schemes for one-dimensional modelling should provide means of more complex real-time simulations. Also, high frequency results can be affected by the selected scheme, as some of them are somewhat more diffusive than others and some limiters are more aggressive at fitting inside the second order TVD region, so a study of this influence is also necessary to minimise simulation errors, providing the optimum combination of schemes for a typical simulated turbine.

This work is divided as follows: first, a basic description of the model is shown; second, the different combinations of numerical schemes are benchmarked against CFD data and the results are discussed; finally, the main conclusions are presented.

2. Model description

The radial turbine model that is studied in this work is described in detail in the work by Galindo Lucas et al. [10]. Different parts of the turbine are computed: the turbine inlet, the volute, the stator, the rotor and the turbine outlet.

The turbine inlet and outlet are computed using a one-dimensional, density-based finite volume method. The state vector at each cell is computed using a MUSCL approach [11]: the state vector average value is maintained at each cell and a linear extrapolation is used to compute its value at the cell boundary; the extrapolation slope is limited, however, using a slope limiter function. The volute is also computed using a MUSCL method, and is represented as a convergent duct of the same length and area distribution as the real volute. Each volute cell has additional source terms due to the flow to the stator through its lateral window.

The stator is computed using several non-ideal nozzles connected to the volute cells, coupled with a boundary elements method to estimate its outlet flow angle. The stator produces the source terms for the volute. The rotor is computed as a non-ideal constant rothalpy element, and produces flux terms for the first boundary of the turbine outlet duct.

A scheme of the model is shown in Figure 1. The inlet boundary condition is placed in station 0 and the outlet boundary condition is placed in station 6.

At each time-step, the flux and source terms for the finite volume cells are computed and their state vectors are updated using a standard ODE time integrator. The model presents three degrees of freedom for the selection of the numerical schemes: the time integrator, the slope extrapolation limiter and the inter-cell fluxes approximation function.

Several time-integration schemes have been tested:

1 Explicit Euler scheme (first-order accurate).

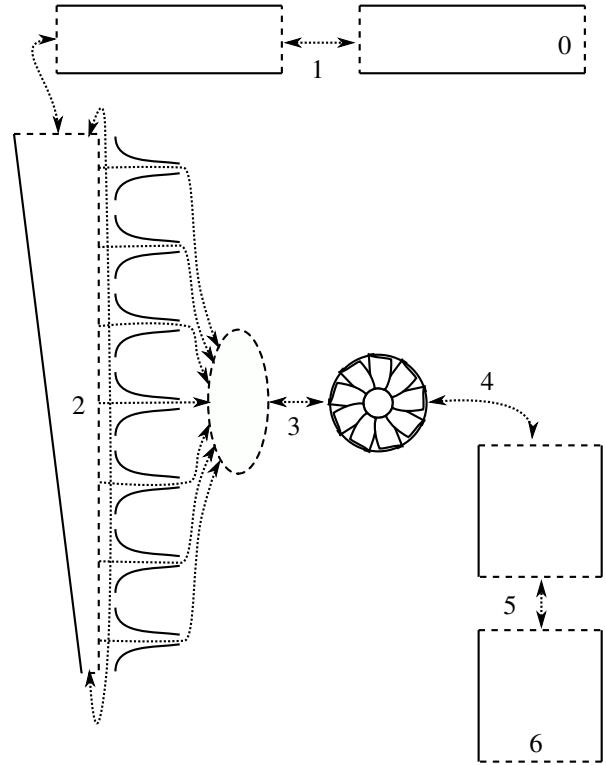


Figure 1: Schematic of the model

- 2 Explicit Heun's method (second-order accurate, two steps).
- 3 Explicit fourth order Runge-Kutta method (fourth-order accurate, four steps).

The last time integrator needs roughly four times the amount of function evaluations as the explicit Euler scheme for a given time-step.

Also, several limiter functions have been tested:

- A Koren.
- B Minmod.
- C MC.
- D Ospre.
- E Superbee.
- F UMIST
- G Van-Albada.
- H Van-Leer.

In this case, the UMIST limiter requires roughly three times the number of function evaluations as the Minmod limiter.

Finally, four different schemes have been used to compute the flux between cells:

- Harten-Lax-Van Leer solver, using a 2 wave approximation of the Riemann fan, see [12].

- Harten-Lax-Van Leer-Contact solver, using a 3 wave approximation of the Riemann fan, see [13].
- Kurganov and Tadmor central scheme, a Riemann-solver free method, see [14].
- Advection Upstream Splitting Method, which divides the flux into two different parts: a convective flux and a pressure flux; see [15].

The Kurganov and Tadmor central scheme requires roughly half the number of function evaluations as the Harten-Lax-Van Leer-Contact approximate Riemann solver.

All the implemented limiters maintain second-order TVD properties, giving second-order spatial accuracy where the state vector is smooth enough and resorting to first-order accuracy in the presence of abrupt gradients and shocks.

All the methods are implemented trying to optimise the locality of the data in order to avoid as much cache misses as possible. Also, all the operations are vectorised, with all the vectors aligned to 128 bit bounds in order to exploit single instruction, multiple data (SIMD) operations of the processor where the simulations are done (in particular, SSSE3 instructions). This way, the differences between the different methods are not only due to the complexity of the mathematical algorithms, but also due to data locality and SIMD exploitability. Whenever a SIMD instruction is executed, two members of a vector can be computed at the same time, as the code uses double precision (64 bit per floating point element). Memoisation has also been used in order to reduce the amount of needed operations at a cost of slightly higher memory consumption. Heap allocations are also avoided whenever possible in favour of stack usage to reduce the overall computational costs. The data is passed as const references between the different functions to avoid copy overheads. Eigen C++ template library for linear algebra [16] has been used for vectorisation.

3. Schemes benchmark

A small automotive radial turbine was simulated using data from an experimental campaign. Figure 2 shows the model results against experimental data and classical volute model results. The sound pressure level of the reflected and transmitted waves are plotted for two different engine speeds and loads (3000 rpm and 50 % of maximum BMEP and 3500 rpm and 100 % of BMEP). The quasi-bidimensional model produces better results for both the reflected and transmitted pressure waves at high frequencies than the classical volute. Two different combinations of inter-cell fluxes approximation and slope extrapolation limiter are shown and, although they produce almost identical results, there are small differences that grow with the frequency and the engine load and speed and, thus, the amplitude of the pulse.

To better test the different schemes, data from an U-RANS CFD campaign is used. The CFD setup, validation and results discussion can be found in [5]. The boundary conditions consisted of an isentropic sinusoidal total pressure wave at station

0 and a constant static pressure at station 6. The different methods are tested with two different inlet boundary condition frequencies: 130 Hz and 750 Hz. The turbine is a radial vaned automotive turbine used in diesel engines with a displacement of 2000 cm³. The rotational speed is set to 180 000 rpm and the mean pressure at the inlet lies at the middle of the turbine operating range. The pulse amplitude is 180 kPa, which is an extremely high value for high frequencies but aids in the characterisation of the subtle result differences between the different schemes. The Courant number is always set at the maximum value that ensures the numerical convergence of the simulation.

The different schemes are tested for errors in the mass flow rate and power output amplitudes. As the mass flow rate and turbine power output have a very strong first harmonic, the pulse amplitude error is used to define the error of the model. Amplitude errors are defined as:

$$\begin{aligned}\Delta\dot{m}_{1,model} &= \dot{m}_{1,model,max} - \dot{m}_{1,model,min} \\ \Delta\dot{m}_{1,RANS} &= \dot{m}_{1,RANS,max} - \dot{m}_{1,RANS,min} \\ \varepsilon_{\Delta\dot{m}_1} &= \frac{\Delta\dot{m}_{1,model} - \Delta\dot{m}_{1,RANS}}{\Delta\dot{m}_{1,RANS}}\end{aligned}\quad (1)$$

$$\begin{aligned}\Delta\dot{W}_{turb,model} &= \dot{W}_{turb,model,max} - \dot{W}_{turb,model,min} \\ \Delta\dot{W}_{turb,RANS} &= \dot{W}_{turb,RANS,max} - \dot{W}_{turb,RANS,min} \\ \varepsilon_{\Delta\dot{W}_{turb}} &= \frac{\Delta\dot{W}_{turb,model} - \Delta\dot{W}_{turb,RANS}}{\Delta\dot{W}_{turb,RANS}}\end{aligned}\quad (2)$$

The subscript *RANS* is for the results of the tridimensional simulation, while *model* is for the results of the simplified model.

The relative speed is defined against the maximum speed obtained for each case.

The differences in accuracy between the different methods are almost negligible at the lowest frequency, and the level of error is indeed almost null with all the tested combinations. At low frequencies, the accuracy of the method is not bounded by the time-integration error, as the CFL condition renders the problem so stiff for explicit schemes that the time-step is low enough even for first-order accurate solvers. At 750 Hz, however, the error of the power amplitude prediction is clearly reduced using a second order scheme, while a fourth order one doesn't produce noticeable improvements and almost doubles the computational time. To get the same level of accuracy at 750 Hz with the first order time-integration scheme, the time-step has to be reduced to levels that induce higher computational costs than that of Heun's method.

The fastest simulation times are obtained using the Minmod limiter or with the VanLeer limiter. The differences in computational time between the different implemented limiters are only of around a couple percent points. The most accurate limiter for mass flow rate estimation appears to be the Minmod limiter, although it is the most conservative in terms of its TVD compliance, but only when used with the HLLC approximate Riemann solver: coupled with the AUSM solver, which is more diffusive than the HLLC solver, it underestimates the amplitude of the

mass flow rate evolution. As with the power output amplitude, however, it is always overestimated and the error is minimised with the AUSM solver. A Pareto optimality is obtained with the KT scheme and the Minmod limiter using Heun’s method, which is also the fastest combination for second order in time.

As a general recommendation, the scheme by Kurganov and Tadmor combined with the Minmod limiter and Heun’s time integration scheme should be used to obtain the best results at the highest frequencies. The HLL approximate Riemann solver gives similar results to KT in the tested cases, but with a 3 % overhead in computational costs. The selected combination of schemes is 10 % faster than the worst-case selection using Heun’s method. If the highest accuracy at high frequencies is not needed, a combination of first order forward Euler method with KT and Minmod should give 80 % extra speed over Heun’s method. The fourth-order, four-steps Runge-Kutta method shows no clear advantage over Heun’s method, so it may be safely discarded.

The authors of this work initially expected higher differences in computational cost between the different schemes. Although some of them required more function evaluations than others, some of them required less CPU cycles due to vectorisation and incurred in less cache misses during the simulation due to better data locality. These effects damped the speed differences between the schemes, although bigger caches and new SIMD instruction sets should reduce this damping in the future.

Figure 4 shows the time-domain results of three different time-integration schemes for the turbine power output for 130 Hz and 750 Hz, using the Minmod limiter function and three different inter-cell fluxes approximations. Although the differences remain small, they are visible in the right-hand-side plot. Due to the stiffness of the equations of the system, explicit schemes must use a small time-step to avoid unstabilities, getting enough accuracy for all the cases except for the highest frequencies. The implemented fourth order Runge-Kutta method incurs in a computational cost penalty too high for its small improvements over the Heun’s method, so the latter one is recommended in cases where very high frequency, extremely high amplitude boundary conditions are expected. If the amplitude for the highest harmonics is low enough, a first order method such as the forward Euler method may be accurate enough. The turbine power output is better reproduced using the AUSM method, while in the case of the mass flow rate (Figure 5) the best amplitude prediction is obtained by the HLLC approximate Riemann solver.

Looking again at Figure 2, there is a difference of a couple of dB between the results of the optimum selection of schemes (KT + Minmod) and a suboptimal selection (AUSM + UMIST), with both cases computed using the same time-step and Heun’s method. The effects of the scheme selection grows with the frequency and, although smaller than the effect of computing the volute using a quasi-bidimensional approach, is still measurable. Although the effect should be bigger for higher frequencies, blade passing and three-dimensional effects are also visible at frequencies higher than 2000 Hz and they are not taken into account in the current model.

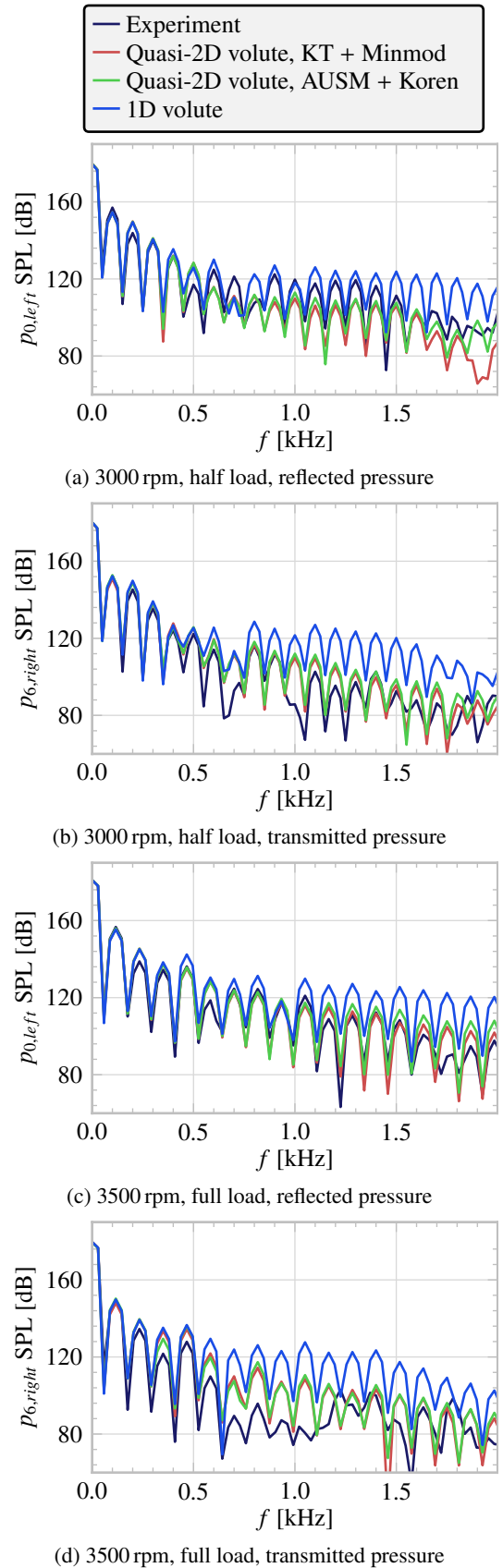
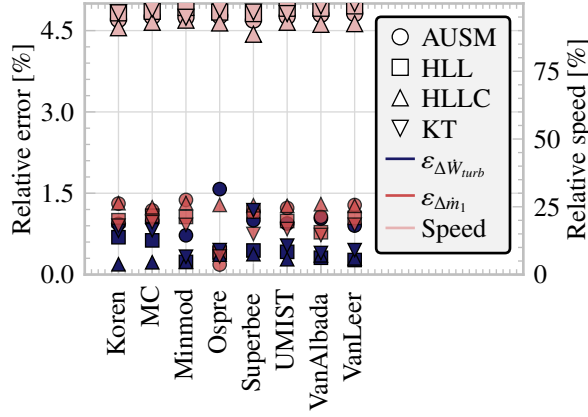
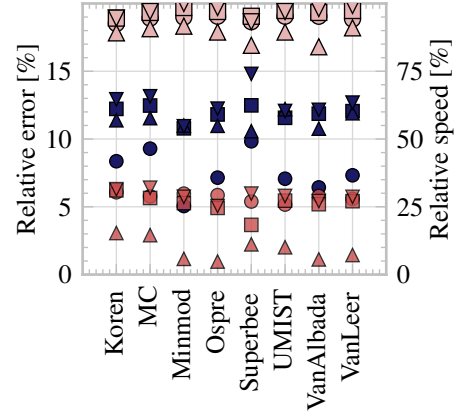


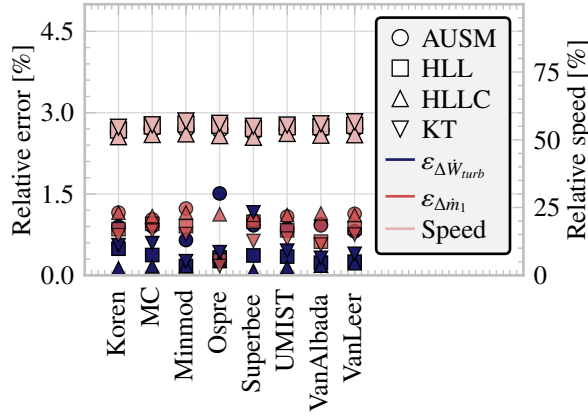
Figure 2: Model results using experimental data



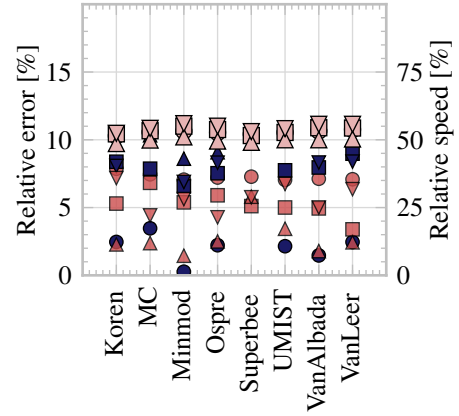
(a) Forward Euler, 130 Hz



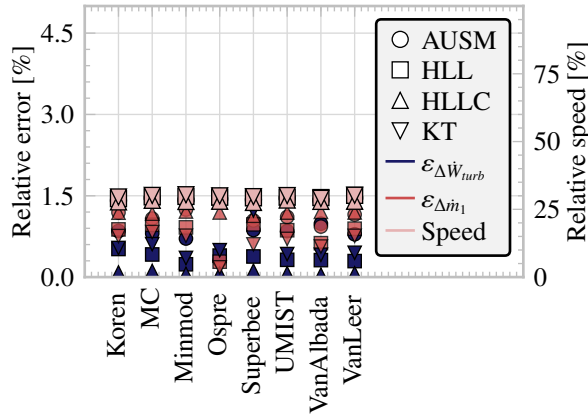
(b) Forward Euler, 750 Hz



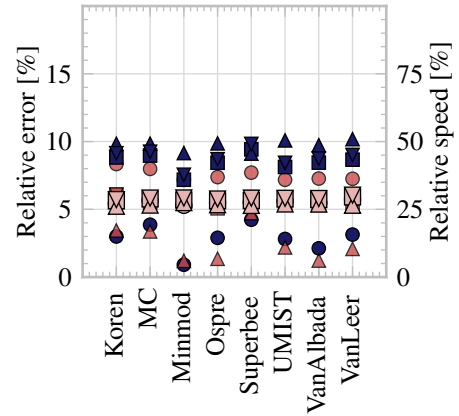
(c) Heun's method, 130 Hz



(d) Heun's method, 750 Hz



(e) Fourth order Runge-Kutta, 130 Hz



(f) Fourth order Runge-Kutta, 750 Hz

Figure 3: Solver test results

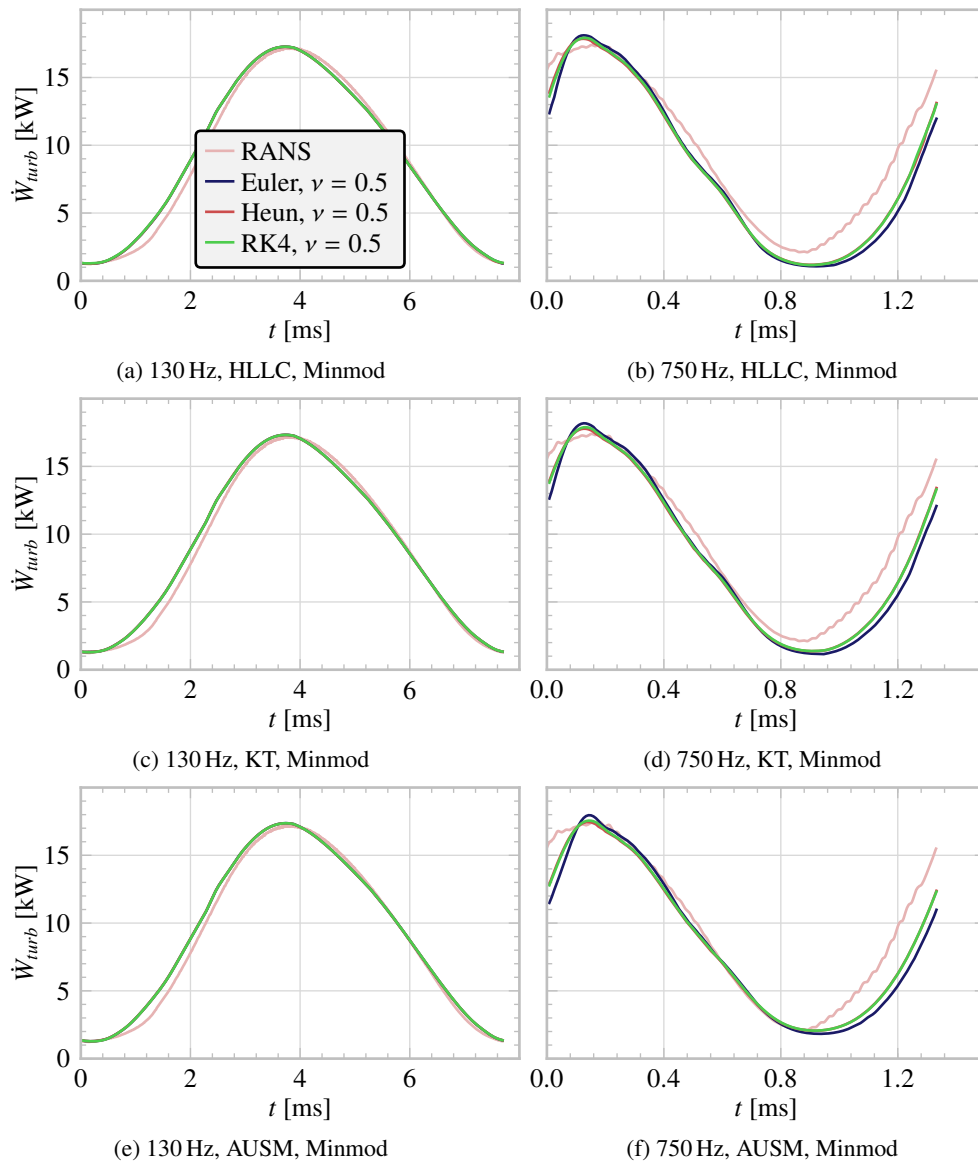


Figure 4: \dot{W}_{turb} , time-integration scheme comparison

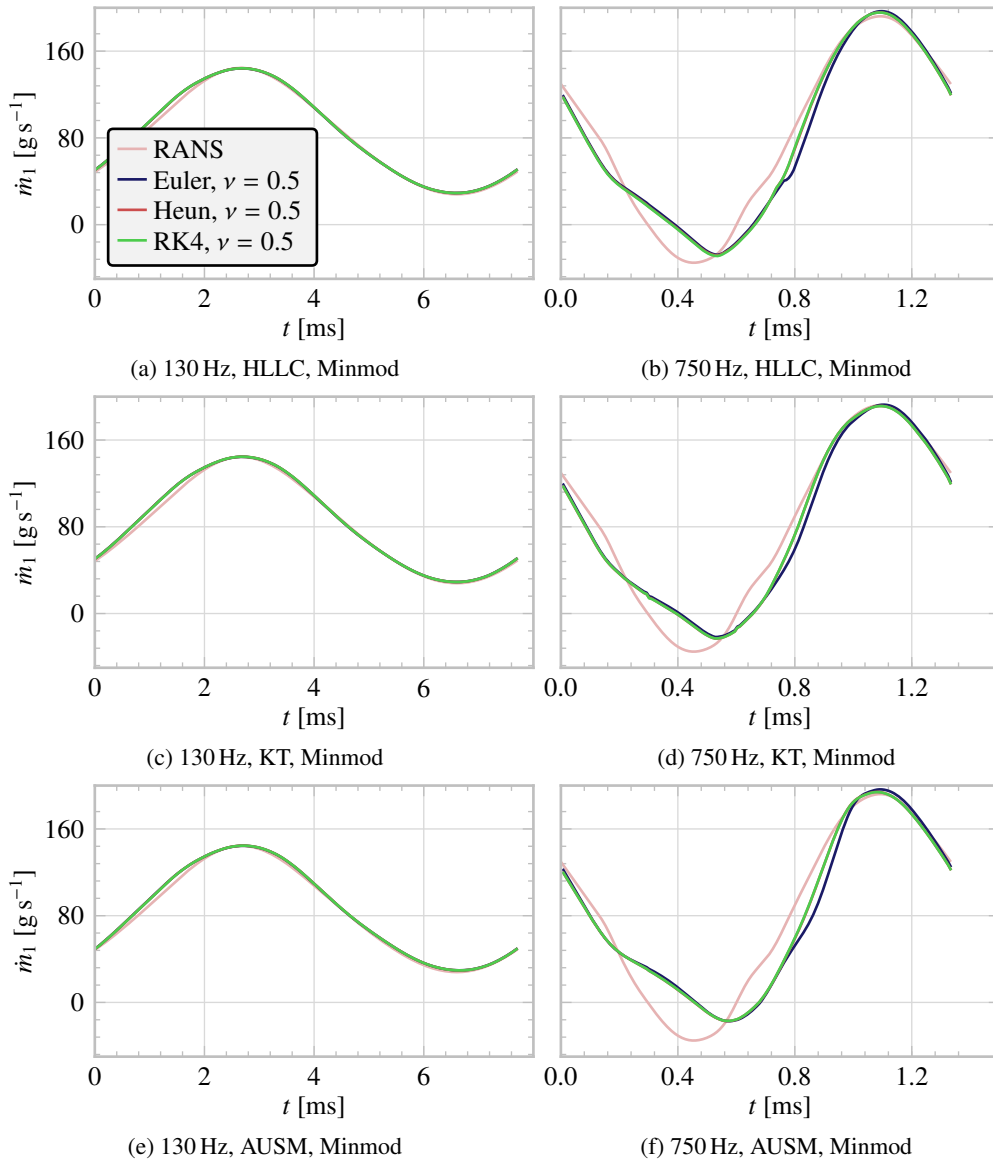


Figure 5: \dot{m}_1 , time-integration scheme comparison

4. Conclusions

This paper presents a study of the influence of several numerical schemes used in the quasi-bidimensional simulation of an automotive radial turbine, using several excitation frequencies for the boundary conditions. The model results are compared with that of U-RANS simulations. The authors have found the following:

- The numerical error due to the discrete time integration is negligible for low frequencies due to the stiffness of the system and the usage of explicit time-integrators. At high frequencies, however, a second-order scheme is needed to produce the most accurate results. No appreciable improvements in the accuracy were found for a fourth order scheme: for a typical spatial mesh size of around 1 cm, the CFL condition renders the time-step low enough and the error is not bounded by the discrete time integration.
- The different inter-cell fluxes approximations and slope limiter functions have different degrees of numerical diffusion and computational cost, so an optimum selection can be performed:
 - At low frequencies, the differences between the different methods are negligible.
 - At high frequencies, Pareto optimality in model error is obtained using the Kurganov and Tadmor central scheme or the Harten-Lax-Van Leer approximate Riemann solver coupled with the Minmod limiter. This also produces the fastest results, with a computational speed-up of around 10 %.
- The authors expected higher computational cost differences between the schemes. The differences in vectorisation and SIMD usage and data locality between the different methods seemed to damp the expected variations in simulation speed. Future processors are expected to give different results, as new instruction sets and larger caches are added.

The model presents noticeable improvements against simulations of a radial turbine using a classic one-dimensional volute approach for frequencies higher than 1000 Hz. The optimum selection of schemes appears to give a couple of dB of extra accuracy against a bad selection for high frequencies. For frequencies higher than 2000 Hz, blade passing and three-dimensional effects should be taken into account to properly compute the turbine non-linear acoustic behaviour and, thus, it is a limit in the accuracy for the presented model. Nevertheless, the limit of accurate prediction of the model is doubled against that of the classical turbine, and the optimum selection of the schemes should be still valid when the model is improved with blade passing and three-dimensional acoustic source terms. The quasi-bidimensional volute model seems to produce an averaging effect in the pressure pulse at the stator inlet that reduces the amplitude of the high frequency spectrum against that of the classical volute.

Acknowledgements

The authors are indebted to the Spanish Ministerio de Economía y Competitividad through Project TRA 2012-36954.

The authors also wish to thank Mr. Roberto Navarro for his invaluable work during CFD simulations.

Nomenclature

CFD	Computational Fluid Dynamics
CFL	CourantFriedrichsLewy
CPU	Central processing unit
FLOP	Floating point operation
\dot{m}	Mass flow rate
MUSCL	Monotonic Upstream-Centered Scheme for Conservation Laws
ODE	Ordinary differential equation
RANS	Reynolds-averaged Navier-Stokes
SIMD	Single instruction, multiple data
TVD	Total variation diminishing
U-RANS	Unsteady Reynolds-averaged Navier-Stokes
\dot{W}	Power

Subscripts

<i>left</i>	Left-travelling wave
<i>model</i>	Model results
<i>RANS</i>	Reynolds-averaged Navier-Stokes
<i>right</i>	Right-travelling wave
<i>turb</i>	Turbine
0	Domain inlet
1	Turbine inlet
2	Stator inlet
3	Stator outlet
4	Rotor outlet
5	Turbine outlet
6	Domain outlet

Greek letters

Δ	Difference
ε	Error
ν	Courant number

References

- [1] European Parliament, Council of the European Union . Regulation (EC) No 715/2007 of the European Parliament and of the Council of 20 June 2007 on type approval of motor vehicles with respect to emissions from light passenger and commercial vehicles (Euro 5 and Euro 6) and on access to vehicle repair and maintenance information (Text with EEA relevance) . Official Journal of the European Union 2007;50:1–16. URL: <http://eur-lex.europa.eu/legal-content/EN/TXT/?uri=OJ:L:2007:171:TOC>.
- [2] European Parliament, Council of the European Union . Regulation (EC) No 595/2009 of the European Parliament and of the Council of 18 June 2009 on type-approval of motor vehicles and engines with respect to emissions from heavy duty vehicles (Euro VI) and on access to vehicle repair and maintenance information and amending Regulation (EC) No 715/2007 and Directive 2007/46/EC and repealing Directives 80/1269/EEC, 2005/55/EC and 2005/78/EC (Text with EEA relevance)

- . Official Journal of the European Union 2009;52:1–13. doi:[10.3000/17252555.L_2009.188.eng](https://doi.org/10.3000/17252555.L_2009.188.eng).
- [3] Payri F, Benajes J, Reyes M. Modelling of supercharger turbines in internal-combustion engines. *Journal of Mechanical Science* 1996;38:835–69. doi:[10.1016/0020-7403\(95\)00105-0](https://doi.org/10.1016/0020-7403(95)00105-0).
 - [4] Baines N, Halijouy-Benisi A, Yeo JH. The pulse flow performance and modelling of radial inflow turbines. In: *Proceedings of the Institution of Mechanical Engineers, 5th International Conference on Turbocharging and Turbochargers*. 1994, p. 209–20.
 - [5] Galindo J, Fajardo P, Navarro R, García-Cuevas LM. Characterization of a radial turbocharger turbine in pulsating flow by means of CFD and its application to engine modeling. *Applied Energy* 2013;103(0):116–27. doi:[10.1016/j.apenergy.2012.09.013](https://doi.org/10.1016/j.apenergy.2012.09.013).
 - [6] Chen H, Winterbone D. A method to predict performance of vaneless radial turbine under steady and unsteady flow conditions. In: *Turbocharging and Turbochargers*. Institution of Mechanical Engineers; 1990, p. 13–22.
 - [7] Abidat M, Hachemi M, Hamidou MK, Baines N. Prediction of the steady and non-steady flow performance of a highly loaded mixed flow turbine. In: *Proceedings of the Institution of Mechanical Engineers*; vol. 212. 1998, p. 173–84. doi:[10.1243/0957650981536844](https://doi.org/10.1243/0957650981536844).
 - [8] Costall AW, McDavid RM, Martnez-Botas RF, Baines NC. Pulse performance modelling of a twin-entry turbocharger turbine under full unequal admission. In: *Proceedings of ASME Turbo Expo 2009*. ASME; 2009,doi:[doi:10.1115/1.4000566](https://doi.org/10.1115/1.4000566).
 - [9] Chiong MS, Rajoo S, Romagnoli A, Martnez-Botas R. Unsteady performance prediction of a single entry mixed flow turbine using 1-d gas dynamic code extended with meanline model. In: *Proceedings of the ASME Turbo Expo*; vol. 5. ASME; 2012, p. 781–95. doi:[10.1115/GT2012-69176](https://doi.org/10.1115/GT2012-69176).
 - [10] Galindo Lucas J, Tiseira Izaguirre A, Fajardo P, García-Cuevas LM. Development and validation of a radial variable geometry turbine model for transient pulsating flow applications. *Energy Conversion and Management* 2014;85(0):190–203. doi:[10.1016/j.enconman.2014.05.072](https://doi.org/10.1016/j.enconman.2014.05.072).
 - [11] van Leer B. Towards the ultimate conservative difference scheme, V. A second order sequel to Godunov’s method. *Journal of Computational Physics* 1979;32:101–36.
 - [12] Einfeld B. On godunov-type methods for gas dynamics. *SIAM J Numer Anal* 1988;25(2):294–318. URL: <http://dx.doi.org/10.1137/0725021>.
 - [13] Toro E, Spruce M, Speares W. Restoration of the contact surface in the hll-riemann solver. *Shock Waves* 1994;4(1):25–34. URL: <http://dx.doi.org/10.1007/BF01414629>.
 - [14] Kurganov A, Tadmor E. New high-resolution central schemes for nonlinear conservation laws and convection-diffusion equations. *J Comput Phys* 2000;160(1):241–82.
 - [15] Liou MS, Steffen Jr. CJ. A New Flux Splitting Scheme. *Journal of Computational Physics* 1993;107(1):2339. doi:[10.1006/jcph.1993.1122](https://doi.org/10.1006/jcph.1993.1122).
 - [16] Guennebaud G, Jacob B, et al. Eigen v3. <http://eigen.tuxfamily.org>; 2010. Last visited on 2013/10/23.